frontiers | Frontiers in Earth Science

TYPE Original Research
PUBLISHED 18 March 2024
DOI 10.3389/feart.2024.1361620

OPEN ACCESS

EDITED BY
Faming Huang,
Nanchang University, China

REVIEWED BY
Jiulong Ding,
Xi'an University of Technology, China
Zhilu Chang,
Nanchang University, China

*CORRESPONDENCE
Qi Wan,
wanqi77@163.com
Xiaohua Yang,
xiaohauy@126.com

RECEIVED 26 December 2023
ACCEPTED 27 February 2024
PUBLISHED 18 March 2024

CITATION
Wan Q, Yang X, Wang R and Zhu Z (2024), Dynamic deformation and meso-structure of coarse-grained saline soil under cyclic loading with freeze-thaw cycles.
Front. Earth Sci. 12:1361620.
doi: 10.3389/feart.2024.1361620

Dynamic deformation and meso-structure of coarse-grained saline soil under cyclic loading with freeze-thaw cycles

Qi Wan[1,2,3]*, Xiaohua Yang[2]*, Rui Wang[4] and Zhiheng Zhu[1,3]

[1]Guangdong Transportation Technology Testing Co., Ltd, Guangzhou, Guangdong, China, [2]School of Highway, Chang'an University, Xi'an, Shaanxi, China, [3]Guangdong HuaLu Transportation Technology Co., Ltd, Guangzhou, Guangdong, China, [4]School of Civil Engineering, Chang'an University, Xi'an, Shaanxi, China

The cumulative deformation properties of subgrade soil under cyclic traffic loads are critical for optimizing pavement structure design and ensuring long-term highway structural performance. This study aims to investigate the coupling effect of freeze-thaw cycles and cyclic loads on the cumulative deformation behaviors and meso-structure of coarse-grained saline soil (CGSS) subgrade filling in high-cold areas. Dynamic triaxial tests and computed tomography (CT) scanning were conducted to analyze the CGSS under different working conditions. The research focused on the dynamic deformation development and damage evolution under varying freeze-thaw cycles and load amplitudes. The research results show that the cumulative deformation behavior of CGSS under cyclic loading is relatively sensitive to the freeze-thaw process. The cumulative dynamic strain increases as the freeze-thaw cycles, with a critical freeze-thaw cycle number of five. The stable cumulative dynamic strain curve exhibits clear three-stage characteristics when plotted in semi-log coordination, with critical loading cycles at 20 and 1,000. After 10–100 loading cycles, the cumulative strain curve quickly shows failure. The CGSS's low density and pore regions greatly increase after a freeze-thaw cycle. The rise in dynamic stress amplitude notably affects the bonding between soil particles and crystalline salts. The coupling effect of the freeze-thaw cycle and dynamic activity exacerbates the deterioration of soil structure, resulting in variations in CT values within the scanning layer in the final state.

KEYWORDS

subgrade, dynamic triaxial test, freeze-thaw cycle, accumulated deformation, coarse-grained saline soil, meso-structure

1 Introduction

The Qarhan Salt Lake, situated in the southern Qaidam Basin of the Qinghai-Tibet Plateau, is the largest inland salt lake in China. With the promotion of China's Belt and Road Initiative in the alpine region, coarse-grained saline soil (CGSS) has been widely used as subgrade and structural materials in highway construction (Yang et al., 2020; Ran et al., 2022). Many studies and empirical cases have shown that the strength and deformation parameters of subgrade soil differ

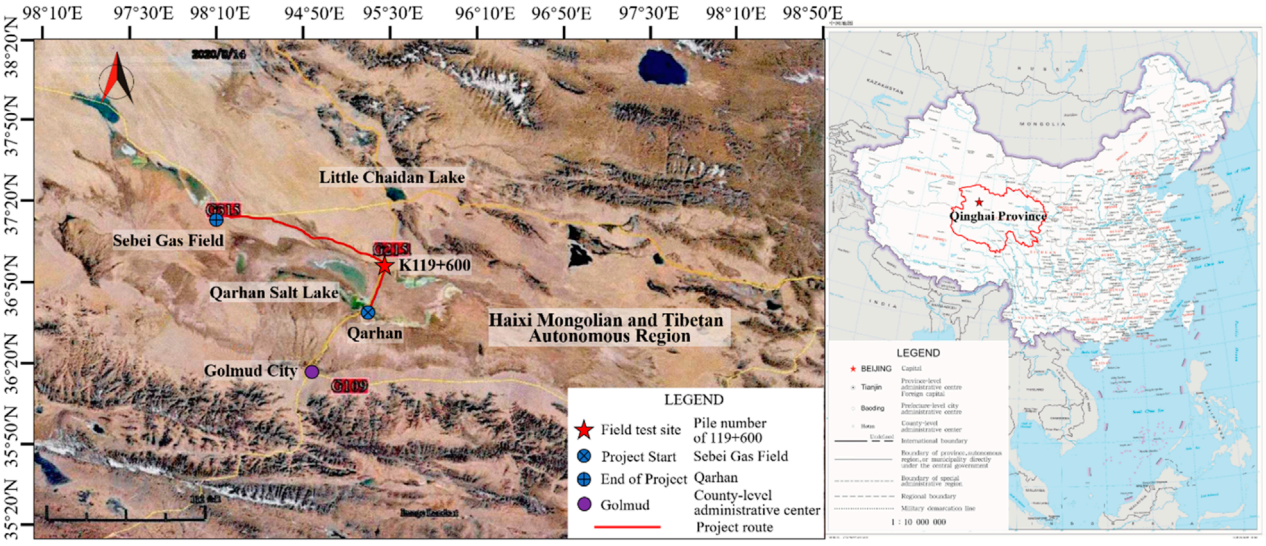

FIGURE 1
Geographic location of the Sebei-Qarhan Highway (G215) project and sampling site.

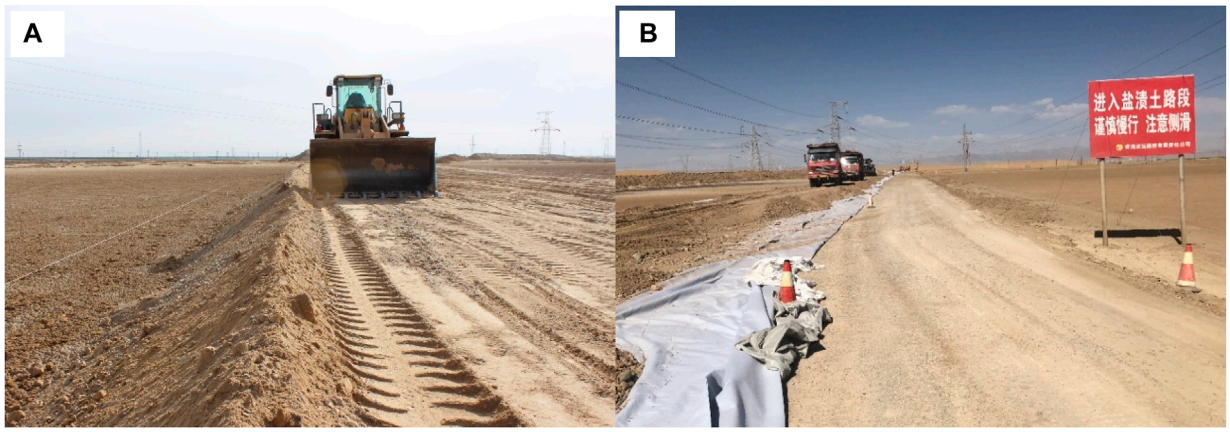

FIGURE 2
Subgrade filling. **(A)** subgrade compaction **(B)** saline soil road section.

significantly under cyclic loading conditions compared to static loading (Shahu et al., 2000; Guo et al., 2013a; Wang et al., 2022; Zheng et al., 2022). Soil failure strength under dynamic loading conditions is significantly reduced compared to static strength. Xie (2011) demonstrated through research that soils, especially those with unique engineering characteristics, show deformation induced by vibrations when exposed to long-term dynamic loads with small amplitudes. In subgrade saline soil, the presence of salt and water phases can significantly alter the internal soil structure. Under cyclic dynamic stress, soil particles experience significant displacement, rotation, and deformation, leading to catastrophic failure in engineering applications, which significantly affects subgrade stability. The freeze-thaw cycle alters the physical and mechanical properties of saline soil by continuously converting between liquid and salt phases (Sun et al., 1980; Wang et al., 2018; Wang et al., 2020). As a result, the subgrade saline soil has always been affected by freeze-thaw cycles due to the temperature differential between day and night, which varies depending on the season (Xu et al., 2021). Highway construction in the Qarhan salt lake area is impacted by freeze-thaw cycles, leading to varying degrees of strength damage and performance degradation in the subgrade. This poses a serious threat to the security of highway operations. Worldwide climate warming has exacerbated the significant temperature differences in high-cold salt lake areas. The saline soil subgrade structure will be more vulnerable to uneven settlement, pavement structure damage, and other issues due to the combination of long-term dynamic loads and freeze-thaw cycles. Therefore, it is crucial to have a comprehensive understanding of the dynamic response of coarse-grained saline soil (CGSS) concerning the coupling effect of freeze-thaw cycles and cyclic traffic loads.

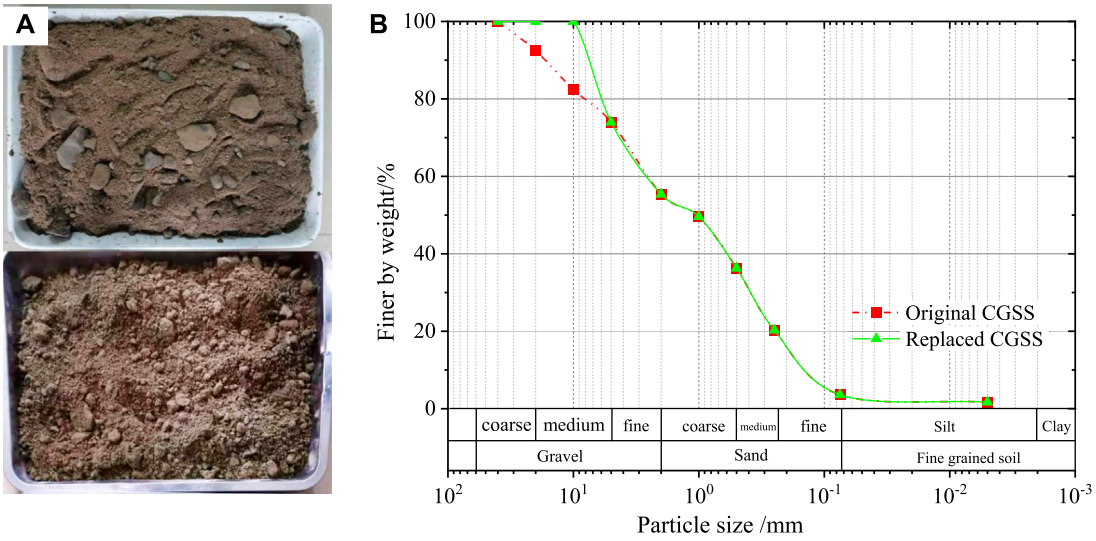

FIGURE 3
Particle size distribution. **(A)** grading curve **(B)** soil samples before and after replacement.

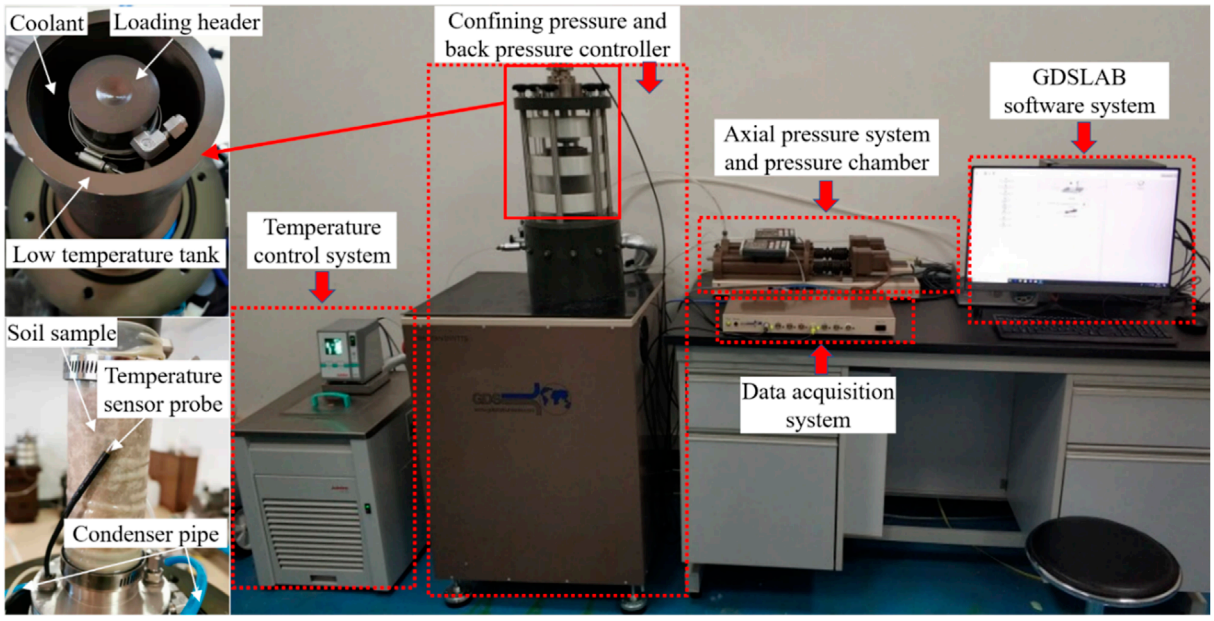

FIGURE 4
GDS dynamic triaxial test system.

Currently, research on the dynamic response characteristics of soil during freeze-thaw cycles is mostly centered on multi-year and seasonal frozen soil regions. Xu et al. (2021) conducted dynamic triaxial tests on the frozen soil of the Qinghai Tibet highway under different freeze-thaw cycles and proposed a plastic cumulative strain prediction model. Fan et al. (2021) investigated the effects of freeze-thaw cycles and dynamic loads on dynamic mechanical characteristics and cumulative permanent strain of frozen soil through dynamic triaxial tests. Zhang et al. (2019) studied the effect of different coarse particle contents on dynamic modulus and damping ratio of frozen soil in cold regions, and modified the Monismith model by studying the development law of cumulative plastic strain. Yang et al. (2019) studied the changes in dynamic shear modulus and damping ratio of expansive soil under freeze-thaw cycling conditions through temperature controlled dynamic triaxial tests. Wang et al. (2017) studied the dynamic stress-strain curves and strain rates of red sandstone samples in high-cold regions under different freeze-thaw cycles, and analyzed deformation and failure processes under freeze-thaw cycles and impact loads using energy loss ratios. Zhu et al.

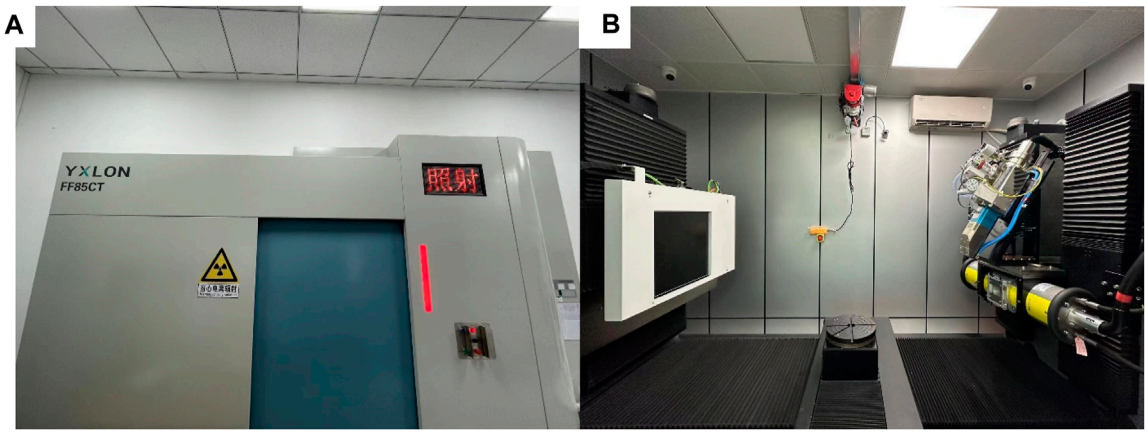

FIGURE 5
High resolution industrial CT System. **(A)** YXLON FF85 CT **(B)** Inside X-ray protection cabinet.

(2010) studied the changes in residual strain of frozen soil of the Qinghai Tibet Railway under the influence of temperature, water content, and confining pressure based on low-temperature dynamic triaxial tests, and established a settlement prediction model under long-term traffic loads. Xiao et al. (2018) tested the effects of thawed frozen soil on the dynamic performance of pile structures and analyzed the vibration properties of the system using the frequency spectrum.

It can be seen that a lot of research has been done on the dynamic characteristics of frozen soil under the coupling effect of the freeze-thaw cycle process and cyclic load. However, the development of dynamic deformation and damage evolution of CGSS subgrade fillers is a subject that has received limited research attention. Meanwhile, studies on saline soils mostly focus on the frost heave and the salt heave deformation mechanism of sulfate saline soils (Yang et al., 2017; Yu et al., 2019), the dissolution deformation characteristics of chloride saline soils (Wei et al., 2014; Yu et al., 2019), and the basic properties of carbonate saline soils (Wang et al., 2011). Zhang et al. (2019) utilized a hollow cylindrical torsion shear apparatus to investigate the dynamic cumulative strain development law of sulfuric acid saline soil in heavy-haul railway subgrade under coupled loads of positive and horizontal cyclic stresses in terms of dynamic characteristics. Zhao et al. (2020) studied the pore distribution characteristics and micro-mechanisms of saline soil under traffic loads. However, the dynamic behavior of saline soil in high-cold regions under traffic loads during freeze-thaw cycles is not taken into account.

The primary objective of this study is to investigate the freeze-thaw effect on the dynamic deformation behaviors of the CGSS subgrade fillers obtained from the Sebei-Qarhan Highway in the Qarhan Salt Lake area. Dynamic triaxial tests were performed on the CGSS subgrade fillers that had undergone multiple freezing and thawing cycles (0–7 times). Firstly, in light of the test results, the dynamic response of the CGSS subgrade fillers that underwent different freeze-thaw cycles was investigated, and the critical freeze-thaw cycle number for achieving the steady state of the dynamic properties of the CGSS subgrade fillers was determined. Secondly, the cumulative dynamic strain characteristics under long-term traffic loading were analyzed, and an accumulative model was proposed to describe the accumulated deformation of CGSS subgrade fillers under the influence of freeze-thaw cycles. Finally, CT scanning tests were conducted to reveal the mechanism of strength degradation of CGSS subgrade fillers under the combined influence of freeze-thaw cycles and traffic loads from a microscopic perspective.

2 Materials and methods

2.1 Test soil sample

The Qarhan Salt Lake area is situated in the hinterland of the Qinghai-Tibet Plateau in Qinghai Province. It belongs to the typical plateau continental climate. Due to the high-cold environmental conditions, rich salt-bearing host rocks, and strong weathering, the chlorine saline soil is well-developed in the Qarhan Salt Lake area,

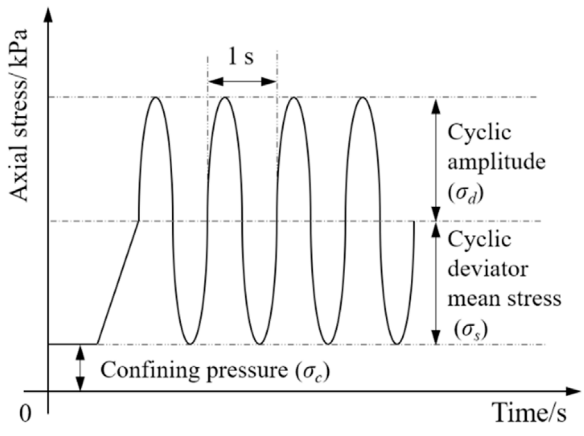

FIGURE 6
Schematic of sinusoidal axial loading process.

TABLE 1 Loading conditions.

Test soil sample	Load frequency (Hz)	Confining pressure σ_c (kPa)	Dynamic stress amplitude σ_d (kPa)	Freeze-thaw cycles	Loading number
CGSS	1.0	20	0, 20, 40, 60, 90, 120, 150, 200	0, 1, 3, 5, 7	10,000

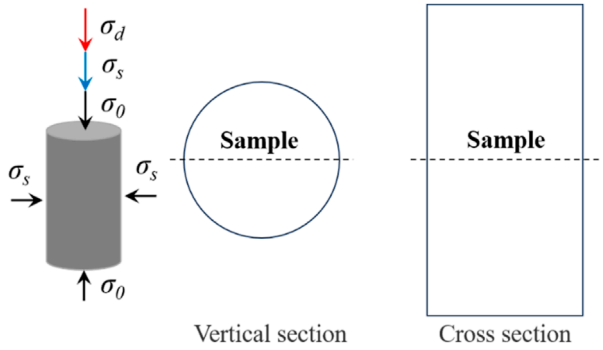

FIGURE 7
Scanning position.

with an occurrence thickness of more than 20 m. The tested soil samples studied in this experiment were taken from the construction site of the K119 + 600 section of the Sebei-Qarhan Highway (G215), which is one of the first highways built in the Qarhan Salt Lake area (refer to Figures 1, 2). The maximum particle size of the original soil does not exceed 40.0 mm, and the non-uniformity coefficient (C_u) and curvature coefficient (C_c) are 23.3 and 1.58, respectively.

In order to ensure consistency between the tested soil sample and subgrade filling, a triaxial sample was prepared following the Test Methods of Soils for Highway Engineering (Ministry of Communications of the People's Republic of China, 2020). A standard cylinder with a diameter of 50 mm and a height of 100 mm was utilized for this purpose. The maximum particle size of the sample was 10 mm. To prevent the influence of oversized particles on the test results, groups of particles with equal mass (particle size range 5–10 mm) were utilized to substitute for oversized particles (larger than 10 mm) in proportion. This not only ensures the skeletal structure of coarse particles in the soil but also maintains the content of other particle groups unchanged, preserving the continuity of the original soil grading. The particle grading curves of the soil samples before and after replacement are illustrated in Figure 3. According to the laboratory tests, the maximum dry density and optimal moisture content of the soil sample are 2.17 g/cm^3 and 6.8%, respectively, with a salt content of 3.0%. It belongs to the chloride type of moderately saline soil.

2.2 Test instruments

The equipment used in this dynamic triaxial test is the temperature-controlled bidirectional vibration triaxial test system (DYNTTS) produced by GDS company in the United Kingdom. It mainly includes a power drive device, back pressure and confining pressure controller, temperature control system, and data acquisition device, as shown in Figure 4. The main technical indicators and parameters are as follows: the axial load range is 0–60 kN, the confining pressure control range is 0–20 MPa, the loading frequency range is 0–10 Hz, the axial displacement limit is ±100 mm, and the temperature range is N.T.P. (Normal Temperature and Pressure) to −30°C. The temperature is controlled by a refrigeration compression circulator, and the freeze-thaw cycle process of saline soil is achieved by continuously regulating the temperature of the frozen liquid within the pressure chamber through it.

The computed tomography (CT) is a highly accurate non-destructive testing technique. Its principle is to reflect the internal structure of an object by comparing the intensity before and after X-ray incidence, without damaging or changing the tested object. Generally, the higher the material density, the stronger the absorption ability of X-rays, and the greater the brightness displayed on CT images (Zhu et al., 2015; Hu et al., 2018). The CT scanning tests were performed using the YXLON FF85 CT, an innovative and versatile high-resolution CT system, as depicted in Figure 5. The sample scanning accuracy used in this detection test is 39 μm.

2.3 Experiment scheme

This research area features a typical plateau continental climate, with an altitude ranging from 2,680 to 2,800 m. The average temperature from January to April and September to December is below zero, with a historical minimum temperature of −36°C. The temperature from May to August ranges from 5°C to 15°C, with the highest temperature reaching 25°C. The temperature at night in summer ranges from −3°C to −5°C, with a significant difference in temperature between day and night. To simulate the freeze-thaw cycle caused by large temperature differences in the context of global warming and humidifying climate trends in high-altitude salt lake regions, this experiment controlled the minimum temperature at −25°C and the maximum temperature at 25°C, with a temperature reduction and heating rate of 0.1°C per minute. A significant body of literature suggests that for specific types of soil, when the freeze-thaw cycle surpasses 10 times, the trend of soil strength attenuation decreases significantly and stabilizes (Wang et al., 2017; Wang et al., 2020; Fan et al., 2021; Xu et al., 2021). Due to the excessively long freeze-thaw cycle test, conducting each cycle test from 0 to 10 times will span

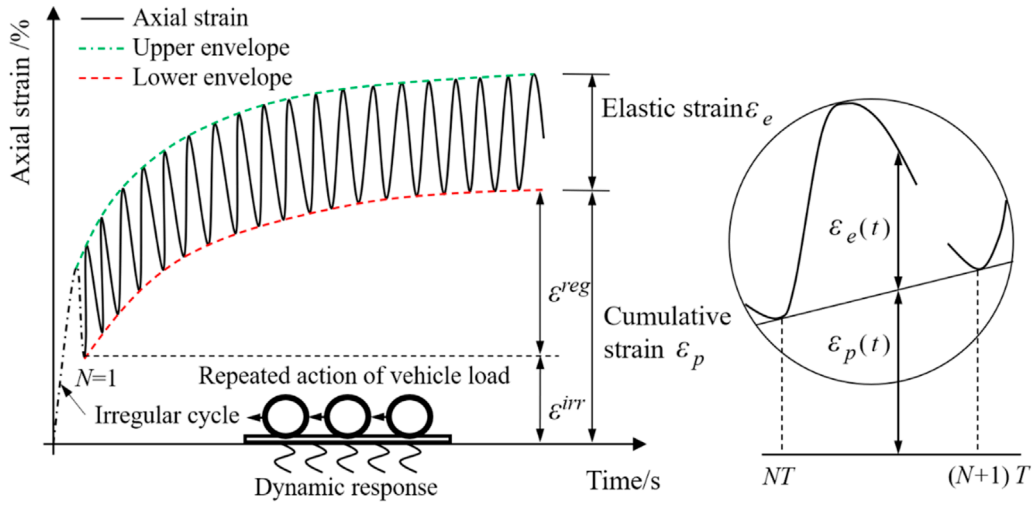

FIGURE 8
Schematic diagram of cumulative strain calculation in dynamic cyclic tests.

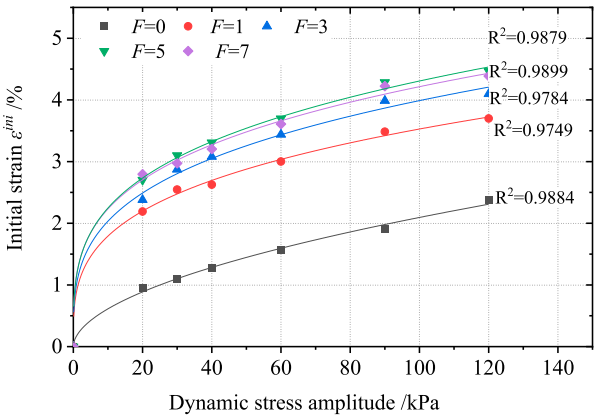

FIGURE 9
Changes in initial strain under different freeze-thaw cycles.

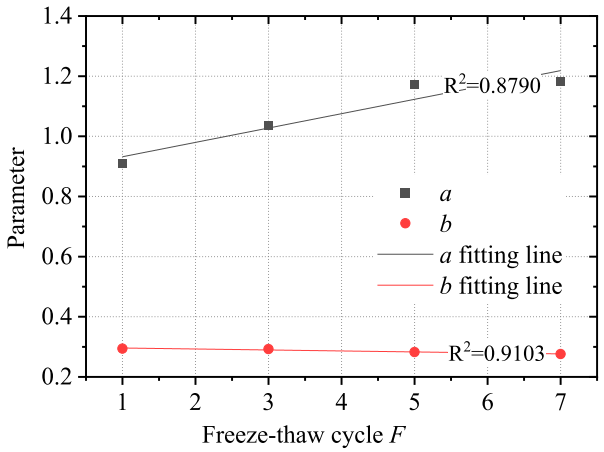

FIGURE 10
The variation of parameters *a* and *b* with the number of freeze-thaw cycles.

different seasons, leading to significant temperature variations in the indoor test environment and causing substantial errors in the test results. Therefore, to ensure the comprehensiveness of the test plan and the timeliness of the test results, the numbers of freeze-thaw cycles in this test have been set to 0, 1, 3, 5, and 7, based on the initial stage test results and conclusions drawn from numerous references, and the freezing and melting processes each continued for 12 h, simulating one freeze-thaw cycle.

Considering the impact on the natural ecological environment of the salt lake area, the entire route of the Sebei-Qarhan Highway is designed based on the principle of low embankment and gentle slope, with a height range of 1.0–1.5 m. When the volume-weight of the fill is 20 kN/m^3, the soil confining pressure ranges from 10 to 30 kPa. Therefore, the confining pressure in the dynamic triaxial test is 20 kPa. Considering the limitations posed by complex geological and construction conditions, the compaction degree of CGSS is controlled at 0.92. As shown in Figure 6, the sinusoidal loading waveform is applied to the unidirectional pulse and continuous stress of the soil within the subgrade under vehicle load. Here, σ_c represents the confining pressure, σ_s denotes the static deviator stress, and σ_d indicates the cyclic stress amplitude. In order to simulate the long-term effect of vehicle load on the subgrade soil, the test is completed when the loading number reaches 10,000 times or the axial strain reaches 12%, with a load frequency of 1.0 Hz and a dynamic stress amplitude of 20–200 kPa, as listed in Table 1.

In order to clearly describe the mechanism of long-term performance degradation of the CGSS subgrade under the coupling effect of climate change and traffic loading, the typical samples of triaxial tests were analyzed by selecting the CT images from both transversal and longitudinal sections, as shown in Figure 7.

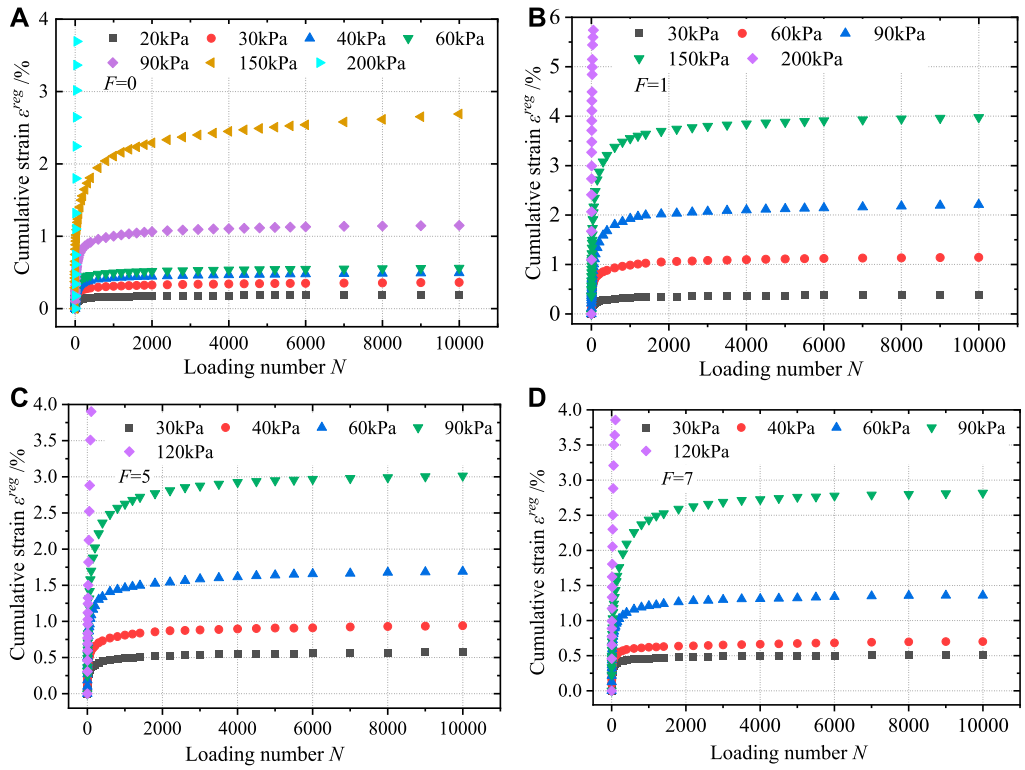

FIGURE 11
The cumulative strain variation with different freeze-thaw cycles. **(A)** Freeze-thaw cycle F = 0 **(B)** Freeze-thaw cycle F = 1 **(C)** Freeze-thaw cycle F = 5 **(D)** Freeze-thaw cycle F=7.

The changes in micro parameters of the internal soil structure under freeze-thaw cycles and cyclic loads are primarily studied. In consideration of the integrity of soil structure, samples subjected to dynamic stress amplitudes of 30 kPa, 60 kPa, and 90 kPa are being analyzed.

3 Analysis of test results

3.1 The effect of freeze-thaw cycles on initial strain

The results indicate that the sample undergoes a significant initial strain after the first cyclic loading (N = 1), and the consistency of this strain is low, which is much smaller than the strain generated by subsequent cyclic loading (N > 1), as shown in Figure 8. Therefore, when analyzing the cumulative strain law of CGSS, the development of strain is divided into two stages based on the loading number: first, the initial strain (ε^{ini}) generated under the first load; second, the regular cumulative strain (ε^{reg}) generated by subsequent loads. Thus, the cumulative plastic strain can be expressed as the sum of ε^{irr} and ε^{reg}, as follows:

$$\varepsilon_p = \varepsilon^{irr} + \varepsilon^{reg} \tag{1}$$

Figure 9 shows the variation of initial strain with dynamic stress amplitude for different freeze-thaw cycles (F). Previous studies have shown that freeze-thaw cycles have a significant impact on soil structure (Liu et al., 2016; Lu et al., 2016; Wang et al., 2020; Xu et al., 2021; Yang et al., 2021). From the figure, it can be seen that the initial strain increases non-linearly with dynamic stress. After the first freeze-thaw cycle, the initial strain increases by 1.16–1.33 times. When the number of freeze-thaw cycles is 5 and 7, the difference in initial strain between the two is very small. Using a power function to fit the initial strain under different freeze-thaw cycles, the parameters "a" and "b" exhibit a linear relationship with F (Figure 10), as depicted in fitting Eq. 2.

$$\varepsilon^{irr} = a \times {\sigma_d}^b$$

$$a = 0.8840 + 0.04774F;\ b = 0.2994 - 0.00326F \tag{2}$$

3.2 The effect of freeze-thaw cycles on cumulative strain

Figure 11 illustrates the variation of cumulative strain with dynamic stress amplitude for different freeze-thaw cycles (F). It can be seen that both dynamic stress amplitude and temperature (freeze-thaw cycle) have a significant impact on the cumulative plastic strain (Zhang et al., 2016). The cumulative strain curve of the failure mode sharply increases within 100 loading cycles, leading

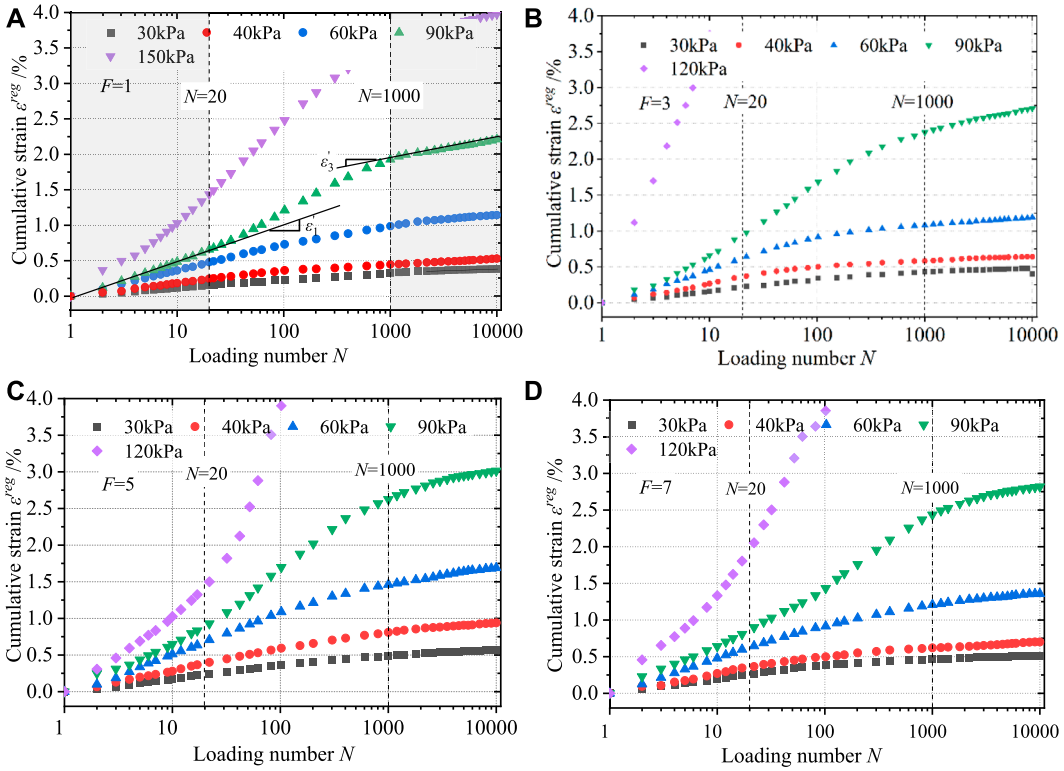

FIGURE 12
Cumulative strain variation in semi logarithmic coordinates. **(A)** Freeze-thaw cycle *F* = 1 **(B)** Freeze-thaw cycle *F* = 3 **(C)** Freeze-thaw cycle *F* = 5 **(D)** Freeze-thaw cycle *F*=7.

to rapid failure. When the freeze-thaw cycle ranges from 0 to 1, the critical dynamic stress for sample failure is between 150 kPa and 200 kPa. When the freeze-thaw cycle ranges from 3 to 7, the critical dynamic stress ranges from 90 kPa to 120 kPa. When the number of freeze-thaw cycles is 5 and 7, the cumulative deformation curves under the same dynamic stress amplitude are very close, which is consistent with the experimental results of the initial strain. Meanwhile, the critical dynamic stress varies greatly under different freeze-thaw cycles. When the freeze-thaw cycle in the initial phase (0–1 times), The critical dynamic stress range for specimen failure is 150–200 kPa. When the freeze-thaw cycle reaches 3–7 times, the critical dynamic stress range for specimen failure is 90–120 kPa.

Figure 12 illustrates the variation of cumulative strain of CGSS with different freeze-thaw cycles under semi-logarithmic coordinates. It can be observed that the stable cumulative strain curve under different freeze-thaw cycles exhibits a three-stage characteristic. The cumulative strain at different stages is fitted using a logarithmic function, as shown in Eq. 3.

$$\varepsilon^{reg} = f(F,\sigma_d,N) = \begin{cases} k_1\sigma_d lgN, 0 \le N \le 20 \\ k_3\sigma_d + k_2\sigma_d lgN, 1000 \le N \end{cases}$$
$$k_1 = 0.00371 + 0.00266F - 0.00039F^2$$
$$k_2 = 0.00134 + 0.00126F - 0.00023F^2$$
$$k_3 = 0.00925 + 0.00273F - 0.00023F^2 \quad (3)$$

Based on the triaxial cyclic test of compacted loess conducted by Wang (2019), it was observed that the cumulative strain under long-term, low-intensity cyclic loading shows an increasing trend when plotted on a semi-logarithmic coordinate system. This observation implies a significant difference in the evolution of strength properties between fine-grained and coarse-grained soils when exposed to long-term cyclic traffic loads. This difference can be attributed to the varying mechanical properties resulting from the distinct soil structures. In saline soil, the freeze-thaw cycle process significantly alters the original internal soil structure. Therefore, the subgrade soils endure not only numerous cyclic loads that are below the shear strength but also the detrimental effects of freeze-thaw cycles, ultimately leading to significant deformations in the subgrade (Zhou et al., 2016; Xu et al., 2020; Xu et al., 2021).

3.3 Analysis of damage evolution based on CT scanning

The principles of CT scanning imaging and the CGSS samples after the triaxial test are shown in Figures 13, 14. After passing through the material, variances in X-ray intensity are produced due to differences in attenuation, which are then captured at the receiving terminal. Then, the changes in radiation intensity are converted into CT value variations through detectors, computers, etc., and represented in grayscale values

FIGURE 13
CGSS samples of triaxial tests.

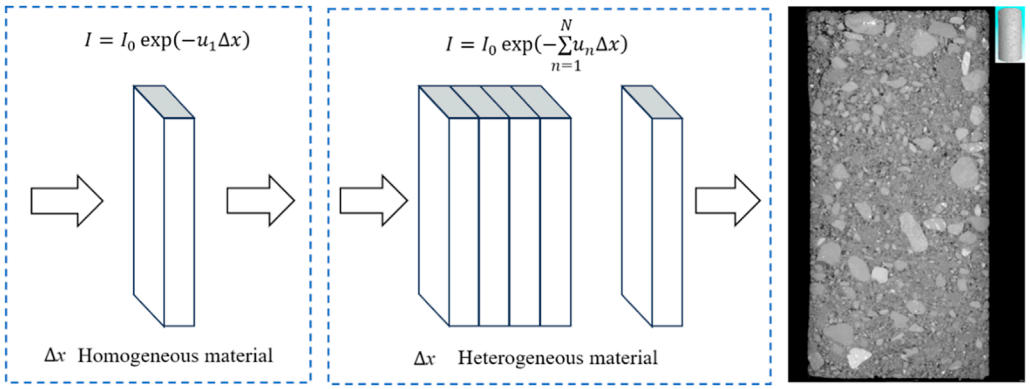

FIGURE 14
Principles of CT scanning imaging.

on the image. The attenuation law they proposed satisfies Eq. 4 (Yao et al., 2021).

$$I = I_0 \exp\left(-u_m \rho X\right)$$

$$u = u_m \rho \tag{4}$$

Where I and I_0 are the light intensity before and after X-ray irradiation; u_m is the unit mass absorption coefficient of the tested sample, ρ is the density of the tested sample; X is the length of ray penetration; u is the attenuation coefficient of a line passing through a tested sample of 1 cm.

Due to the differences in X-ray absorption among different materials, the CT value represents the material's ability to absorb X-rays, which can determine the density status of the material. Hounsfield proposed the following definition for the CT value (Hounsfield, 1973):

$$H_\rho = \frac{u - u_m}{u_w} \times 1000 \tag{5}$$

Where H_ρ is the CT value of the scanned sample; u_w is the absorption coefficient of water ($u_w = u_w$, H_ρ=0, i.e. u_w can be used as the CT standard value).

Figure 15 displays scanning images of CGSS samples under various sections and test conditions, illustrating the soil structure's condition under different freeze-thaw cycles and cyclic loads. Figures 15A,B show the CT images without undergoing freeze-thaw cycles (F = 0) and with dynamic stress amplitudes of 30 kPa and 60 kPa. After 10,000 loading cycles, numerous pores and small internal cavities appear on various sections of the CGSS samples, with no cracks, and the initial damage is not readily apparent. When the number of freeze-thaw cycles is 1, and the dynamic stress amplitude remains at 60 kPa, the number of pores in the section increases, and local transverse cracks appear. When the number of freeze-thaw cycles increases to 3 and 5, the cracks in the central area of sample sections develop significantly. Additionally, when the dynamic stress amplitude increases to 90 kPa, the sample exhibits significant lateral deformation, with the central part showing a drum shape. When the number of freeze-thaw cycles reaches 7, the crack width rapidly expands, forming a Y-shaped crack throughout the sample. When the number of freeze-thaw cycles is 5 and 7, the damaged area is very similar, which aligns with the findings of the dynamic triaxial test.

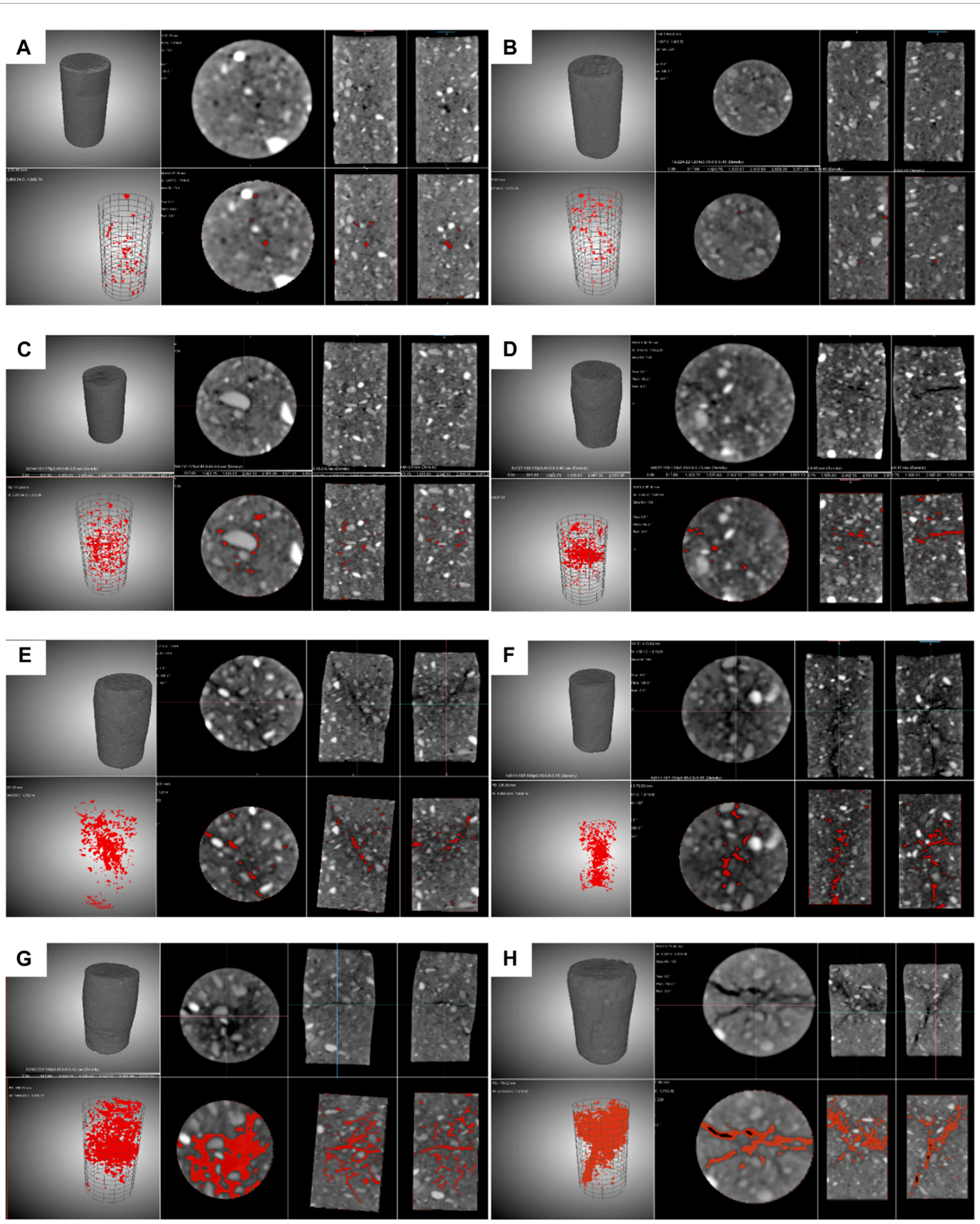

FIGURE 15
Effects of freeze-thaw cycles and cyclic loads on pore development in specimens. **(A)** $F = 0$, $\sigma_d = 30$ kPa **(B)** $F = 0$, $\sigma_d = 60$ kPa **(C)** $F = 1$, $\sigma_d = 30$ kPa **(D)** $F = 1$, $\sigma_d = 60$ kPa **(E)** $F = 3$, $\sigma_d = 60$ kPa **(F)** $F = 5$, $\sigma_d = 60$ kPa **(G)** $F = 5$, $\sigma_d = 90$ kPa **(H)** $F = 7$, $\sigma_d = 90$ kPa.

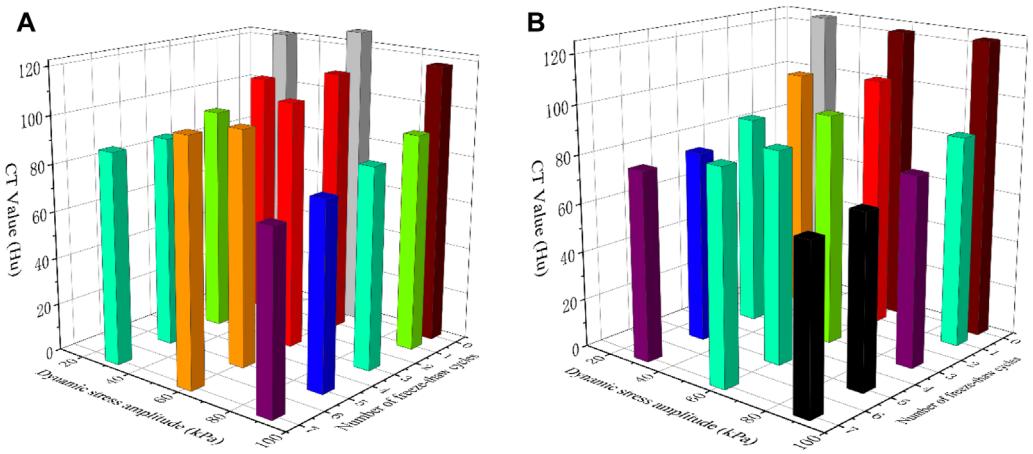

FIGURE 16
CT values of each scanning section under different working conditions. **(A)** Sample central part (cross-section) **(B)** Sample axial plane (vertical-section). (Unit: Hu).

TABLE 2 CT damage variable values.

Dynamic stress amplitude σ_d (kPa)	CT damage variable value D				
	$F = 0$	$F = 1$	$F = 3$	$F = 3$	$F = 5$
0	1.021	1.352	1.953	2.119	2.123
60	1.232	1.653	2.487	2.506	2.498
90	1.347	2.104	2.883	2.924	2.903

The CT value can reflect the average density of geotechnical materials, and its variation reflects the damage to the internal structure. As the degree of internal defect development increases, the average CT value decreases. The CT values of the central (cross-sectional) and axial (vertical-sectional) surfaces of samples under different working conditions were obtained from the scanning test. From Figure 16, it can be seen that there is a significant difference in CT values among different scanning sections under various working conditions. The CT value without freeze-thaw cycles is around 120 Hounsfield units (Hu), and the CT value is highest when the dynamic stress amplitude is 60 kPa.

This indicates that without freeze-thaw cycles, the soil continues to be compacted under dynamic loads, and the compaction deformation between soil particles is much greater than the lateral deformation. When the number of freeze-thaw cycles is 1, the CT value rapidly decreases. With a dynamic stress amplitude of 30 kPa, the CT value decreases by 18.55%, and with a dynamic stress amplitude of 90 kPa, the CT value decreases by 29.27%. It can be observed that the CT value of the cross-section is typically sensitive to freeze-thaw cycles. This sensitivity suggests that the freeze-thaw cycle process can notably decrease the soil's compactness, resulting in deformation and failure under dynamic loads. Under the same number of freeze-thaw cycles, when the amplitude of dynamic stress increases from 60 kPa to 90 kPa, the CT value of the cross-section decreases by 16.35%–21.84%, and the CT value of the vertical section decreases by 17.86%–26.47%. Under the same dynamic stress amplitude, as the dynamic stress amplitude increases, the CT value on the scanning section continues to decrease. The degree of decrease in the cross-section is greater than that in the vertical section. When the number of freeze-thaw cycles is 5 and 7, the CT values of the transverse and vertical sections are relatively close, which is consistent with the results of the cyclic dynamic triaxial test. This indicates that during the dynamic triaxial test, the CT value on the vertical section of the sample is more sensitive to the increase in dynamic load, while the CT value on the cross-section is more sensitive to the early freeze-thaw effect.

To quantify the coupling effect of freeze-thaw cycles and dynamic load on CGSS performance, the CT damage variable D can be used for analysis, as shown in Eq. 6 (Hu et al., 2018).

$$D = \frac{1}{m_0^2}\frac{\rho_0 - \rho}{\rho_0} = \frac{1}{m_0^2}\frac{\Delta\rho}{\rho_0} \tag{6}$$

Where m_0 is the spatial resolution; $\Delta\rho$ is the density change value of the scanning layer; ρ_0 is the initial density value of the material.

According to Table 2, under the same freeze-thaw cycle, the dynamic stress amplitude increases from 60 kPa to 90 kPa, and

the damage variable value D increases by 9.3%–27.3%. When the dynamic stress amplitude is 60 kPa, the number of freeze-thaw cycles F increases from 0 to 7, and the damage variable value D increases by 1.02 times. This indicates that cyclic loading continuously enhances the expansion and connectivity of cracks between soil particles after freeze-thaw cycles, which is also the main reason for the possible cracking of the subgrade during long-term service.

4 Conclusion

This paper analyzes the impact of different freeze-thaw cycles on the long-term performance of coarse-grained saline soil in high-cold salt lake areas under cyclic loading, focusing on both macro and meso aspects. The main conclusions are as follows.

(1) The freeze-thaw cycle process has a significant impact on the long-term deformation of CGSS under cyclic loading. The axial cumulative dynamic strain of the sample increases notably with the rise in freeze-thaw cycles, with the critical freeze-thaw cycle number being 5.

(2) The cumulative dynamic strain of CGSS under semi-logarithmic coordinates exhibits a three-stage characteristic as cyclic loading times increase. Two critical loading times are identified at N = 20 and N = 1,000. A three-fold line can be employed to establish a prediction model for the cumulative strain of CGSS subgrade fillers influenced by freeze-thaw cycles.

(3) The variation pattern of CT values can reflect the internal damage situation. A lower CT value corresponds to a more advanced degree of defect development. During the dynamic triaxial test process, the CT value on the vertical section is more sensitive to the increase in dynamic load, while the CT value on the cross-section is more responsive to the early freeze-thaw cycle effect.

(4) With the same freeze-thaw cycle, an elevation in dynamic stress amplitude leads to a 9.3%–27.3% escalation in the damage variable value D. Specifically, when the dynamic stress amplitude is 60 kPa, and the number of freeze-thaw cycles increases from 0 to 7, the damage variable value D, increases by a factor of 1.02.

Data availability statement

The original contributions presented in the study are included in the article/supplementary material, further inquiries can be directed to the corresponding authors.

Author contributions

QW: Methodology, Writing–original draft. XY: Resources, Writing–original draft. RW: Supervision, Writing–review and editing. ZZ: Validation, Writing–review and editing.

Funding

The author(s) declare financial support was received for the research, authorship, and/or publication of this article. The studies presented in the paper were supported by the National Science Foundation of China (Grant No. 52078496) and the project of Ministry of Transport of the People's Republic of China (Safety Emergency Digital Control System and Platform Demonstration Based on Highway Infrastructure Monitoring and Early Warning).

Conflict of interest

Authors QW and ZZ were employed by Guangdong Transportation Technology Testing Co., Ltd, Guangdong HuaLu Transportation Technology Co., Ltd.

The remaining authors declare that the research was conducted in the absence of any commercial or financial relationships that could be construed as a potential conflict of interest.

Publisher's note

References

Fan, C.-X., Zhang, W.-D., Lai, Y., and Wang, B.-X. (2021). Mechanical behaviors of frozen clay under dynamic cyclic loadings with freeze-thaw cycles. *Cold Reg. Sci. Technol.* 181, 103184. doi:10.1016/j.coldregions.2020.103184

Guo, L., Wang, J., Cai, Y.-Q., Liu, H.-L., Gao, Y.-F., and Sun, H.-L. (2013a). Undrained deformation behavior of saturated soft clay under long-term cyclic loading. *Soil Dyn. Earthq. Eng.* 50 (1), 28–37. doi:10.1016/j.soildyn.2013.01.029

Hounsfield, G. N. (1973). Computerized transverse axial scanning (tomography): part 1. description of system. *Br. J. Radiol.* 46 (552), 1016–1022. doi:10.1259/0007-1285-46-552-1016

Hu, H.-X., Duan, X.-L., He, Z.-M., Yang, Y., and Liu, Y.-X. (2018). Mechanical properties and meso mechanical performance evaluation of coarse-grained soil fillers based on dynamic triaxial CT test China. *J. Highw. Transp.* 31 (11), 42–50. http://zgglxb.chd.edu.cn/CN/Y2018/V31/I11/42

Liu, J.-L., Chang, D., and Yu, Q.-M. (2016). Influence of freeze-thaw cycles on mechanical properties of a silty sand. *Eng. Geol.* 210, 23–32. doi:10.1016/j.enggeo.2016.05.019

Lu, Y., Liu, S.-H., Weng, L.-P., Wang, L.-J., Li, Z., and Xu, L. (2016). Fractal analysis of cracking in a clayey soil under freeze–thaw cycles. *Eng. Geol.* 208, 93–99. doi:10.1016/j.enggeo.2016.04.023

Ministry of Communications of the People's Republic of China (2020). *Test methods of soils for highway engineering: JTG 3430-2020*. Beijing: China Communications Press.

Ran, W.-P., Wang, J.-S., Li, L., and Chen, H.-M. (2022). Laboratory test and prediction model of dynamic resilient modulus of coarse-grained sulfate saline soil. *J. Hunan Univ. Nat. Sci.* 49 (3), 154–166. doi:10.16339/j.cnki.hdxbzkb.2022036

Shahu, J. T., Yudhbir Rao, N. S. V. K., and Kameswara Rao, N. (2000). A rational *method* for design of railroad track foundation. *Soils Found.* 40 (6), 1–10. doi:10.3208/sandf.40.6_1

Sun, J.-L., Wang, S.-Z., Bai, L.-T., and Zhang, Z.-C. (1980). An analysis of the stability of railway in chaerhan saline Lake Area. *J. Beijing Univ. Technol.* 6 (3), 52–65. https://journal.bjut.edu.cn/bjgydxxb/cn/article/id/3eae9e14-086a-4dc2-b177-9cdc698fe32e

Wang, C., Lai, Y.-M., Yu, F., and Li, S.-Y. (2018). Estimating the freezing-thawing hysteresis of chloride saline soils based on the phase transition theory. *Appl. Therm. Eng.* 135, 22–33. doi:10.1016/j.applthermaleng.2018.02.039

Wang, J.-Q., Wang, Q., Kong, Y.-Y., Han, Y., and Cheng, S.-K. (2020). Analysis of the pore structure characteristics of freeze-thawed saline soil with different salinities based on mercury intrusion porosimetry. *Environ. Earth Sci.* 79, 161. doi:10.1007/s12665-020-08903-w

Wang, P., Xu, J.-Y., Fang, X.-Y., and Wang, P.-X. (2017). Energy dissipation and damage evolution analyses for the dynamic compression failure process of red-sandstone after freeze-thaw cycles. *Eng. Geol.* 221, 104–113. doi:10.1016/j.enggeo.2017.02.025

Wang, R. (2019). *The dynamic response and long-term strength and settlement of loess railway embankment subjected to train load*. Xi'an: Chang'an University Press, 000004. doi:10.26976/d.cnki.gchau.2019

Wang, R., Hu, Z.-P., Ren, X., Li, F.-T., and Zhang, F. (2022). Dynamic modulus and damping ratio of compacted loess under long-term traffic loading. *Road. Mater. Pavement Des.* 23 (8), 1731–1745. doi:10.1080/14680629.2021.1924232

Wang, W.-H., Wang, Q., Zhang, J., and Chen, H.-E. (2011). An experiment study of the fundamental property of the carbonate-saline soil in west of Jilin province. *J. Beijing Univ. Technol.* 37 (02), 217–224. https://journal.bjut.edu.cn/bjgydxxb/cn/article/id/a1a43a08-3c7c-49ae-b3d9-459dde6e569d

Wei, J., Du, Q.-W., and Feng, C.-X. (2014). Melt sinking and salt-heaving characteristics of coast chlorine saline soil. *J. Chang'an Univ. Nat. Sci.* 34 (4), 13–19. doi:10.19721/j.cnki.1671-8879.2014.04.003

Xiao, F., Chen, G.-S., Hulsey, J. L., Davis, D., and Yang, Z.-H. (2018). Characterization of the viscoelastic effects of thawed frozen soil on pile by measurement of free response. *Cold Reg. Sci. Technol.* 145, 229–236. doi:10.1016/j.coldregions.2017.09.011

Xie, D. Y. (2011). *Soil dynamics*. Beijing: Higher Education Press.

Xu, X.-T., Li, Q.-L., and Xu, G.-F. (2020). Investigation on the behavior of frozen silty clay subjected to monotonic and cyclic triaxial loading. *Acta Geotech.* 15, 1289–1302. doi:10.1007/s11440-019-00826-6

Xu, X.-T., Zhang, W.-D., Fan, C.-X., Lai, Y., and Wu, J. (2021). Effect of freeze–thaw cycles on the accumulative deformation of frozen clay under cyclic loading conditions: experimental evidence and theoretical model. *Road. Mater. Pavement Des.* 22 (4), 925–941. doi:10.1080/14680629.2019.1696221

Yang, S.-L., Zhang, W., Wen, Y., and Li, B. (2017). Salt expansion and lateral mechanical properties of fine-grained saline soil foundation in Xining basin. *J. Qinghai Univ. Nat. Sci.* 35 (6), 61–68. doi:10.13901/j.cnki.qhwxxbzk.2017.06.011

Yang, X.-H., Zhang, S.-S., Liu, W., and Yu, Z.-L. (2020). Research progress on engineering properties of coarse-grained saline soil. *J. Traffic. Transp. Eng.* 20 (05), 22–40. doi:10.19818/j.cnki.1671-1637.2020.05.002

Yang, Z.-N., Lv, J.-H., Shi, W., Jia, C., Wang, C., Hong, Y., et al. (2021). Experimental study of the freeze thaw characteristics of expansive soil slope models with different initial moisture contents. *Sci. Rep.* 11, 23177. doi:10.1038/s41598-021-02662-9

Yang, Z.-N., Zhang, L., Ling, X.-Z., Li, G.-Y., Tu, Z.-B., and Shi, W. (2019). Experimental study on the dynamic behavior of expansive soil in slopes under freeze-thaw cycles. *Cold Reg. Sci. Technol.* 163, 27–33. doi:10.1016/j.coldregions.2019.04.003

Yao, J.-K., Chen, X.-B., Cai, D.-G., Hu, H., Xie, K., and Wu, M.-L. (2021). Characterization analysis of meso-structure of coarse-grained soil filling based on X-ray CT. *Railw. Eng.* 61 (5), 70–74. doi:10.3969/j.issn.1003-1995.2021.05.16

Yu, T.-Y., Wu, Y.-P., Liao, J., and Pu, Z.-G. (2019). Experimental Study on collapse characteristics of sandy chlorine saline soil in Qinghai province. *Sci. Technol. Eng.* 19 (18), 276–281. http://www.stae.com.cn/jsygc/article/abstract/1810446?st=article_issue

Yu, T.-Y., Wu, Y.-P., Si, P.-G., Zhang, L., Kong, L.-G., and Pu, Z.-G. (2019). Experimental study of salt-frost heave characteristics of fine-grained sodium sulfate saline soil. *J. Glaciol. Geocryol.* 41 (2), 407–441. doi:10.7522/j.issn.1000-0240.2019.0060

Zhang, D., Li, Q.-M., Liu, E.-L., Liu, X.-Y., Zhang, G., and Song, B. (2019). Dynamic properties of frozen silty soils with different coarse-grained contents subjected to cyclic triaxial loading. *Cold Reg. Sci. Technol.* 157, 64–85. doi:10.1016/j.coldregions.2018.09.010

Zhang, J.-X., Lin, G.-H., Wang, Y.-X., and Jiang, P.-L. (2019). Experimental study on dynamic behavior of sulphate soil subgrade under cyclic loading. *Earthq. Eng. Eng. Vib.* 39 (2), 27–34. doi:10.13197/j.eeev.2019.02.27.zhangjx.004

Zhang, S., Tang, C.-A., Hu, P., Zhang, X.-D., and Zhang, Z.-C. (2016). Reversible and irreversible strain behavior of frozen aeolian soil under dynamic loading. *Environ. Earth. Sci.* 75, 245. doi:10.1007/s12665-015-5009-z

Zhao, F.-T., Chang, L.-J., and Zhang, W.-Y. (2020). Analysis on the influence of cyclic stress ratio and vibration frequency on microstructure of saline soil. *J. Glaciol. Geocryol.* 42 (3), 854–864. doi:10.7522/j.issn.1000-0240.2020.0065

Zheng, D.-H., Tang, L.-S., Wang, Y.-X., and Sun, Y.-L. (2022). Dynamic stress accumulation effects on soil strength under cyclic loading. *Soils Found.* 62 (4), 101164. doi:10.1016/j.sandf.2022.101164

Zhou, Z.-W., Ma, W., Zhang, S.-J., Du, H.-M., Mu, Y.-H., and Li, G.-Y. (2016). Multiaxial creep of frozen loess. *Mech. Mater.* 95, 172–191. doi:10.1016/j.mechmat.2015.11.020

Zhu, B.-L., Wu, X.-Y., Li, X.-N., and Wei, J.-P. (2015). Triaxial CT tests of meso-structure evolution of remodeled cohesive soil in Hefei. *J. Southwest Jiaot. Univ.* 50 (1), 144–149. doi:10.3969/j.issn.0258-2724.2015.01.021

Zhu, Z.-Y., Ling, X.-Z., Chen, S.-J., Zhang, F., Wang, L.-N., Wang, Z.-Y., et al. (2010). Experimental investigation on the train-induced subsidence prediction model of Beiluhe permafrost subgrade along the Qinghai–Tibet Railway in China. *Cold Reg. Sci. Technol.* 62 (1), 67–75. doi:10.1016/j.coldregions.2010.02.010